


## Discrimination of Ohmic thermal baths by quantum dephasing probes

Alessandro Candeloro<sup>\*</sup> and Matteo G. A. Paris<sup>†</sup>*Quantum Technology Lab, Dipartimento di Fisica Aldo Pontremoli, Università degli Studi di Milano, I-20133 Milano, Italy*
 (Received 20 August 2020; accepted 24 December 2020; published 21 January 2021)

We address the discrimination of structured baths at different temperatures by dephasing quantum probes. We derive the exact reduced dynamics and evaluate the minimum error probability achievable by three different kinds of quantum probes, namely, a qubit, a qutrit, and a quantum register made of two qubits. Our results indicate that dephasing quantum probes are useful in discriminating low values of temperature and that lower probabilities of error are achieved for intermediate values of the interaction time, where the minimum probability of error scales as  $1/2N$ , with  $N$  the number of energy levels of the probe. A qutrit probe outperforms a qubit one in the discrimination task, whereas entangled probes show smaller optimal times.

DOI: [10.1103/PhysRevA.103.012217](https://doi.org/10.1103/PhysRevA.103.012217)

### I. INTRODUCTION

Thermometry is about measuring the thermodynamic temperature of a system. In classical thermodynamics, thermometry is based on the zeroth principle, i.e., it relies on the achievable equilibrium between the system and a probe with a much smaller heat capacity. In quantum mechanics, temperature is not an observable in a strict sense. Rather, it is a parameter on which the state of a quantum system may depend. For this very reason, direct measurement of temperature is not available, and one should resort to indirect measurement procedures. During the last decade, quantum thermometric strategies have emerged [1–4], which are mostly based on using external quantum probes interacting with the system under investigation, with the assumption that the interaction between the probe and the system does not change the temperature of the latter. Those strategies, usually termed *quantum probing* schemes, are not based on the zeroth principle, but rather on the engineering of the interaction Hamiltonian, which is exploited to imprint the temperature of the system on the quantum state of the probe. As a matter of fact, quantum probing exploits the inherent fragility of quantum systems against decoherence, turning it into a resource to realize highly sensitive metrological schemes.

In recent years, temperature estimation by quantum probes received much attention [5–14], often using the tools offered by quantum estimation theory. The optimal sensitivity in temperature estimation has been studied for  $N$ -dimensional quantum probes [15] and, more recently, the efficiency of infinite-dimensional quantum probes has been also investigated [16]. The ultimate quantum limits to thermometric precision have been addressed [4], and the use of an out-of-equilibrium quantum thermal machine has been suggested for temperature estimation [17]. Quantum thermometry by dephasing has been also addressed in detail and, in particular,

the performance of single-qubit probes [18] and of quantum registers made of two qubits [19] has been explored.

As a matter of fact, less attention has been devoted to the estimation of a discrete set of temperature values, i.e., to temperature discrimination. The problem is that of telling apart thermal baths with different temperatures, assuming that the possible values of temperature belong to a discrete set  $\{T_1, T_2, \dots\}$  and are known in advance (see Fig. 1 for a pictorial description of the measurement scheme). Indeed, in thermometry there are two main tasks. On the one hand, one may need to estimate the temperature of a sample. On the other hand, there are situations in which the main goal is to monitor the temperature of an object, i.e., to sense any variation of temperature, rather than estimating the temperature itself. In those situations, a sensing device should be characterized by at least two working regimes, and in turn two temperatures, which should be discriminated. This is the

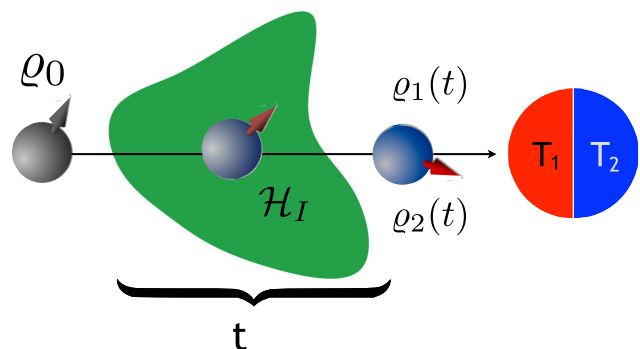


FIG. 1. Discrimination of temperatures by quantum probes. A quantum system prepared in a known state  $\rho_0$  is allowed to interact with a thermal bath for a time  $t$  and then measured in order to discriminate whether the state is  $\rho_1(t)$  or  $\rho_2(t)$ , i.e., to infer whether the temperature of the bath is  $T_1$  or  $T_2$ . After choosing a suitable interaction Hamiltonian  $\mathcal{H}_I$ , the scheme may be optimized over the initial preparation of the probe, and the value of the interaction time  $t$ .

<sup>\*</sup>alessandro.candeloro@unimi.it

<sup>†</sup>matteo.paris@fisica.unimi.it

minimal model we are referring to. Of course, more involved models involving discrimination between a given temperature and *any other temperature* may be devised. In this respect, our analysis provides ways to assess more general monitoring schemes.

In this framework, a single qubit has been suggested [20] as an out-of-equilibrium probe to discriminate two thermal baths and, more recently, the discrimination between baths with different temperatures or statistical properties has been addressed [21], assuming that the quantum probe undergoes Markovian dynamics. In this paper, we extend these studies to more general quantum probes and taking into account the spectral structure of the bath. In particular, we assume a dephasing interaction between the probe and the bath and derive the exact reduced evolution of the quantum probe. Then, we study the discrimination performance of our scheme for different kinds of Ohmic-like environments and different quantum probes. In order to provide a benchmark, we first analyze discrimination by quantum probes at equilibrium, and then address the out-of-equilibrium case, looking for the optimal interaction time, leading to the smallest error probability. Our results indicate that dephasing quantum probes are useful in discriminating low values of temperature and that lower probabilities of error are achieved for intermediate values of the evolution time, i.e., for out-of-equilibrium quantum probes [22].

The paper is structured as follows. In the next section, we review some elements of quantum discrimination theory and establish notation. In Sec. III, we analyze discrimination of thermal baths by quantum probes at equilibrium. Besides being of interest on their own, the results of this section serve as a benchmark to assess the performance of out-of-equilibrium quantum probes, which are analyzed in detail in Sec. IV. Section V closes the paper with some concluding remarks. Throughout the paper we set  $\hbar = 1$ .

## II. THE QUANTUM DISCRIMINATION PROBLEM

In several problems of interest in quantum technology, an observer should discriminate between two or more quantum states. However, quantum states are not observable and this operation cannot be carried out directly. Furthermore, distinct states may have finite overlap, and there is no way to distinguish them with certainty [23]. The main consequence is that a correct discrimination among a generic set of quantum states is not always possible, and an intrinsic error in the process occurs. Many strategies for optimal discrimination of quantum states [24–26] have been suggested, each of them tailored to a specific purpose. In this paper, we are going to use the minimum error discrimination strategy, which we briefly review in the following.

Let us consider the problem of binary discrimination between two quantum states  $\rho_1$  and  $\rho_2$  which are known in advance and occur with *a priori* probability  $\{z_k\}$ ,  $k = 1, 2$ . Given a positive operator-valued measure (POVM)  $\{\Pi_1, \Pi_2\}$ , the quantity  $\text{Tr}[\Pi_j \rho_j]$  represents the probability of correctly inferring the state  $\rho_j$  by implementing the POVM. In order to optimize the discrimination, we look for the POVM minimizing the overall probability of error  $p_e$ , which can be

written as

$$p_e = 1 - \sum_{j=1}^2 z_j \text{Tr}[\Pi_j \rho_j]. \quad (1)$$

Since  $z_1 + z_2 = 1$  and  $\Pi_1 + \Pi_2 = \mathbb{I}$ ,  $p_e$  may be rewritten as  $p_e = z_1 + \text{Tr}[\Lambda \Pi_1] = z_2 - \text{Tr}[\Lambda \Pi_2]$  where the Hermitian operator  $\Lambda$  is defined as

$$\Lambda = z_2 \rho_2 - z_1 \rho_1. \quad (2)$$

Using the spectral decomposition  $\Lambda = \sum_k \lambda_k |\psi_k\rangle\langle\psi_k|$ , the minimum probability of error may be written in terms of the so-called Helstrom bound [27,28]:

$$p_e = \frac{1}{2} \left( 1 - \sum_k |\lambda_k| \right) = \frac{1}{2} (1 - \text{Tr}[|\Lambda|]). \quad (3)$$

Using the distance norm [29] we can interpret the result from a geometrical point of view. Since  $\text{Tr}[|\Lambda|] = \text{Tr}[|z_2 \rho_2 - z_1 \rho_1|] = \|z_2 \rho_2 - z_1 \rho_1\|_1$ , if the occurrence probabilities of  $\rho_1$  and  $\rho_2$  are the same, we obtain

$$p_e = \frac{1}{2} [1 - D(\rho_1, \rho_2)], \quad (4)$$

where  $D(\rho_1, \rho_2) = \frac{1}{2} \|\rho_2 - \rho_1\|_1$  is the trace distance. This result confirms our intuition that the less two states are distant the larger is the probability of error in discriminating them. We also recall that the optimal POVM, for which the probability of error is minimized, is given in terms of the eigenprojectors of the operator  $\Lambda$ , as  $\Pi_1 = \sum_{\lambda_k \leq 0} |\psi_k\rangle\langle\psi_k|$ .

## III. QUANTUM PROBES AT THERMAL EQUILIBRIUM

Let us now turn to the main problem of the paper, i.e., to discriminate whether a thermal bath is at temperature  $T_1$  or  $T_2$  by performing measurements on a quantum probe interacting with it. In this section, we assume that the probe is at the equilibrium with the bath. We do not study how the probe reaches the equilibrium with the bath, and simply assume that after enough time the probe has reached such equilibrium. In the next section, we devote attention to the out-of-equilibrium case and will introduce an interaction model.

Let us consider a quantum system governed by a bounded Hamiltonian  $\mathcal{H}$  with an energy spectrum  $\{|e_n\rangle, E_n\}_{n=0}^{N-1}$ , then the equilibrium state of the probe is given by the Gibbs state

$$\rho_{\text{eq}}(\beta) = \frac{1}{Z(\beta)} \sum_{n=0}^{N-1} e^{-\beta E_n} |e_n\rangle\langle e_n| \quad (5)$$

where  $Z(\beta)$  is the partition function  $Z(\beta) = \sum_n e^{-\beta E_n}$  and  $\beta = 1/T$  (we set the Boltzmann constant to 1 throughout the paper) is the inverse temperature of the heat bath.

Consider now the situation where we do not know in advance the temperature of the bath, but we know it must be  $T_1$  or  $T_2$ . As a result, the thermal state will be different and our goal is to discuss the minimum probability of error in discriminating the two states  $\rho_{\text{eq}}(\beta_1)$  and  $\rho_{\text{eq}}(\beta_2)$ . From the previous section, we know that the best measurement is given

by the operator  $\Lambda$  in (2):

$$\Lambda = \frac{1}{2} \sum_{n=0}^{N-1} \left( \frac{e^{-\beta_2 \frac{\omega_0}{2} \delta_n}}{Z(\beta_2)} - \frac{e^{-\beta_1 \frac{\omega_0}{2} \delta_n}}{Z(\beta_1)} \right) |e_n\rangle \langle e_n|. \quad (6)$$

Then, in the case of  $\beta_2 < \beta_1$ , we have that  $\lambda_0 < 0$  and  $\lambda_1, \dots, \lambda_{N-1} > 0$  and the optimal POVM consists of the projector on the ground state and the projector on any excited state, i.e.,  $\{\Pi_1 = |e_0\rangle \langle e_0|, \Pi_2 = \sum_{n=1}^{N-1} |e_n\rangle \langle e_n|\}$  (if  $\beta_1 < \beta_2$  the role of the projectors in the detection is reversed). If the energy levels are equispaced ( $E_n = \delta_n \omega_0 / 2$  and  $E_{n+1} - E_n = \omega_0$ ), then the probability of error in the discrimination is given by

$$p_e^{\text{eq}}(\beta_1, \beta_2) = \frac{1}{2} - \frac{\text{sgn}(\beta_2 - \beta_1)}{2} \left( \frac{e^{-\beta_2 \frac{\omega_0}{2} \delta_0}}{Z(\beta_2)} - \frac{e^{-\beta_1 \frac{\omega_0}{2} \delta_0}}{Z(\beta_1)} \right). \quad (7)$$

When one of the temperatures is vanishing, say  $T_2 = 0$  ( $\beta_2 = +\infty$ ), the corresponding thermal probe collapses into the ground state  $|e_0\rangle \langle e_0|$  and the probability of error becomes

$$\begin{aligned} p_e^{\text{eq}}(\beta_1, +\infty) &= \frac{1}{2} - \frac{1}{4} \left( \left| \frac{e^{-\beta_1 E_0}}{Z(\beta_1)} - 1 \right| + \sum_{n=1}^{N-1} \left| \frac{e^{-\beta_1 E_n}}{Z(\beta_1)} \right| \right) \\ &= \frac{1}{2} \frac{e^{-\beta_1 E_0}}{Z(\beta_1)}. \end{aligned} \quad (8)$$

In the opposite limit, i.e., when one of the two baths has a very large temperature, say  $T_2$  is very large ( $\beta_2 \rightarrow 0$ ) compared to the largest energy eigenvalue  $\max_n \{E_n\}$ , the corresponding thermal state approaches the equiprobable diagonal state  $\rho_{\text{eq}}(0) = \mathbb{1}/N$ . In this limit, we can easily see that the probability of error scales as the inverse of  $N$ , i.e.,

$$p_e^{\text{eq}} \rightarrow \frac{1}{2N}. \quad (9)$$

For a two-dimensional (qubit) probe  $d = 2$ , a closed formula for (7) may be easily evaluated, obtaining

$$p_e^{\text{eq}}(\beta_1, \beta_2) = \frac{1}{2} \left[ 1 - \frac{1}{2} \left| \tanh \left( \frac{\omega_0 \beta_2}{2} \right) - \tanh \left( \frac{\omega_0 \beta_1}{2} \right) \right| \right]. \quad (10)$$

We will use this expression in the following to compare performance of probes at equilibrium with that of out-of-equilibrium ones.

We now make a few comments on the probability of error (10). The minimum of  $p_e^{\text{eq}}(T_1, T_2)$  depends on the relative choice of  $T_1$  and  $T_2$ . If  $T_2 = 0$ , the minimum is reached asymptotically for  $T_1 \rightarrow +\infty$ , and we know from previous considerations that the limiting value is equal to  $1/4$ . Instead, for  $T_2 > 0$ , we have two cases: if  $T_2 \leq \omega_0 \log(3)$ , the minimum of  $p_e^{\text{eq}}(T_1, T_2)$  is reached for  $T_1 \rightarrow 0$ , while if  $T_2 \geq \omega_0 / \log(3)$  then the minimum of  $p_e^{\text{eq}}(T_1, T_2)$  is again obtained asymptotically for  $T_1 \rightarrow +\infty$ . Moreover, as  $\omega_0$  grows the discrimination improves in the high-temperature regime.

In the rest of the paper and all the subsequent plots, we have set the value of  $\omega_0$  to 3.5 kHz, which corresponds to a realistic experimental situation of a quantum probe [30].

#### IV. OUT-OF-EQUILIBRIUM DEPHASING QUANTUM PROBES

Let us now study how dephasing, out-of-equilibrium, quantum probes may be exploited in the temperature discrimination problem. Here, the quantum probe is an open quantum system  $S$  which effectively interacts with the reservoir, which is a thermal bath at temperature  $T_1$  or  $T_2$ . We assume that the total Hamiltonian of the system is  $\mathcal{H} = \mathcal{H}_0^S + \mathcal{H}_0^B + \mathcal{H}_I$ , where the first term determines the free evolution of the system, the second determines the free evolution of the bath, and the latter determines the interaction between the open quantum system and the reservoir. Before specifying the interaction model, let us discuss some general results about temperature discrimination, regardless of the system and the interaction.

To perform our discrimination task, we prepare our quantum probe in a certain state and then we let it interact with the bath. We assume that the bath is at equilibrium in a Gibbs state:

$$\nu_k = \frac{e^{-\beta_k \mathcal{H}_0^B}}{Z(\beta_k)} \quad (11)$$

where  $\beta_k, k = 1, 2$  are two distinct inverse temperatures. Once the probe state  $\rho_S \equiv \rho_S(0)$  is fixed at time  $t = 0$  and environment state  $\nu_k$ , the evolution of the initially factorized total system  $\rho_S \otimes \nu_k$  is determined by a completely positive trace-preserving (CPT) map  $\Phi_t^k$ . The state of the system at time  $t$  will be

$$\rho_{Sk}(t) = \Phi_t^k[\rho_S] = \text{Tr}_E[U(t) \rho_S \otimes \nu_k U^\dagger(t)]. \quad (12)$$

The two baths at different temperatures define two different CPT maps, and we are going to see that the distance between these two different maps, defined in the last equation, has an upper bound which does not depend on the nature of the probe. The probability of incorrectly discriminating the two states originating from the interaction with the two baths is (4), and it depends on the trace distance  $D(\rho_{S1}(t), \rho_{S2}(t))$ . Since the trace distance is contractive under the action of the trace-preserving map, and invariant under unitary transformations [29,31], we have

$$\begin{aligned} D(\rho_{S1}(t), \rho_{S2}(t)) &= D(\Phi_t^1[\rho_S], \Phi_t^2[\rho_S]) \\ &\leq D(\rho_S \otimes \nu_1, \rho_S \otimes \nu_2) \\ &= D(\nu_1, \nu_2), \end{aligned} \quad (13)$$

where the last equality is due to the fact that the state of the quantum probe at time  $t = 0$  is fixed, regardless of the temperature, and thanks to the additivity under tensor products of the trace distance. Notice that the last equality is no longer true if the states are not factorized. This is an upper bound on the maximum distance between two states evolving under the same reduced dynamics with two baths at  $T_1$  and  $T_2$ . Moreover, this bound depends only on the nature of the bath (namely, its Hamiltonian  $\mathcal{H}_0^B$ ) and on the temperatures to be discriminated. The upper bound translates into a lower bound on the probability of error (4), that is,

$$p_e^{\text{neq}}(T_1, T_2) \geq \frac{1}{2} [1 - D(\nu_1, \nu_2)]. \quad (14)$$

This bound may be useful in dealing with a finite-size environment, whereas in the thermodynamical limit the  $D(\nu_1, \nu_2)$  is likely to vanish.

### A. Dephasing model

In this section we introduce a (pure) dephasing model that regulates the probe-environment interaction by generalizing the qubit model studied in [32]. The full dynamics is generated by the Hamiltonian

$$\mathcal{H}_T = \mathcal{H}_0 + \mathcal{H}_I, \quad (15)$$

where  $\mathcal{H}_0 = \mathcal{H}_0^S + \mathcal{H}_0^B$  determines the free evolution of the probe and the bath, whereas  $\mathcal{H}_I$  describes the interaction. Since we are going to consider quantum probes with a discrete energy spectrum, we may introduce an energy scale  $\omega_0$  to write the energy levels as  $E_n = \delta_n \omega_0 / 2$ . The Hamiltonian may be written as

$$\mathcal{H}_0^S = \frac{\omega_0}{2} \sum_{n=0}^{N-1} \delta_n |e_n\rangle \langle e_n| = \frac{\omega_0}{2} \mathcal{H}^{(n)}. \quad (16)$$

The diagonal matrix  $\mathcal{H}^{(n)}$  represents the spacing of the energy levels, and it may describe the spectrum of a  $n$ -level system, such as qubit  $\mathcal{H}^{(2)} = \sigma_3$ , as well as that of a quantum register of two qubits  $\mathcal{H}^{(2,2)} = (\sigma_3 \otimes \mathbb{I}_2 + \mathbb{I}_2 \otimes \sigma_3)$  [33]. In the second case, the spectrum might be degenerate. Moreover, where appropriate, we understand the index  $n$  as a multi-index  $n = (n_1, n_2)$ , with each  $n_1$  and  $n_2$  associated, respectively, with the first qubit and the second qubit.

The reservoir is described by a bath of harmonic oscillators  $\mathcal{H}_0^B = \sum_k \omega_k b_k^\dagger b_k$ , where  $\omega_k$  are the frequencies of the  $k$ th bosonic modes. Then, the interaction between the system and the reservoir is given by

$$\mathcal{H}_I = \mathcal{H}^{(n)} \otimes \sum_k (g_k b_k^\dagger + g_k^* b_k). \quad (17)$$

The quantities  $g_k$  are the coupling constants between each energy level and the  $k$ th mode of the bath. We assume they do not depend on the energy level with which they interact. This is justified by the assumption that the system is small compared to the size of the reservoir and a collective interaction is a good approximation. In other words, all the energy levels feel the same local environment. Moreover, we assume that in the case of a quantum register all the qubits interact locally with the same thermal bath [19].

The model here is exactly solvable. The evolution of the quantum probe in the interaction picture, given the overall system prepared initially in a factorized state  $\rho_S \otimes \nu$ , is given by

$$\Phi_t^\beta[\rho] = \mathcal{V}^\beta(t) \circ \mathcal{R}(t) \circ \rho_S \quad (18)$$

where the  $\circ$  is the Hadamard (entrywise) product and the quantities  $\mathcal{V}^\beta(t)$  and  $\mathcal{R}(t)$  are given by

$$\mathcal{V}^\beta(t) = \sum_{j,k=0}^{N-1} e^{\frac{(\delta_j - \delta_k)^2}{4} \Gamma(t|\beta)} |e_j\rangle \langle e_k|, \quad (19)$$

$$\mathcal{R}(t) = \sum_{j,k=0}^{N-1} e^{i\xi(t) \frac{\delta_j^2 - \delta_k^2}{4}} |e_j\rangle \langle e_k|. \quad (20)$$

The evolution for a generic quantum probe, initialized in the state  $\rho_S = \sum_{jk} \rho_{jk} |e_j\rangle \langle e_k|$ , is given by

$$\rho_S^\beta(t) = \sum_{jk} \rho_{jk} e^{i\xi(t) \frac{\delta_j^2 - \delta_k^2}{4}} e^{\frac{(\delta_j - \delta_k)^2}{4} \Gamma(t|\beta)} |e_j\rangle \langle e_k|. \quad (21)$$

The functions  $\Gamma(t|\beta)$  and  $\xi(t)$  are defined as follows:

$$\Gamma(t|\beta) = - \sum_k 4 \frac{|g_k|^2}{\omega_k^2} [1 - \cos(\omega_k t)] \coth\left(\frac{\omega_k \beta}{2}\right), \quad (22)$$

$$\xi(t) = -4 \sum_k \frac{|g_k|^2}{\omega_k^2} [\omega_k t - \sin(\omega_k t)]. \quad (23)$$

The first is the decoherence function. It represents the rate of the damping due to the interaction and it depends directly on the temperature. The second one is a temperature-independent phase function which does not affect the probability of error, since the Hadamard product is distributive.

As a final step, we take the continuous limit for the frequency of the bosonic bath, i.e.,  $\sum_k \rightarrow \int d\omega f(\omega)$  and  $|g_k|^2 \rightarrow |g(\omega)|^2$ , where  $f(\omega)$  is the density of states. Upon defining the spectral density as  $J(\omega) = 4f(\omega)|g(\omega)|^2$ , the decoherence function (22) and the temperature-independent phase function (23) become, respectively,

$$\Gamma(t|\beta) = - \int_0^{+\infty} d\omega J(\omega) \coth\left(\frac{\omega \beta}{2}\right) \frac{1 - \cos(\omega t)}{\omega^2}, \quad (24)$$

$$\xi(t) = - \int_0^{+\infty} d\omega J(\omega) \frac{\omega t - \sin(\omega t)}{\omega^2}. \quad (25)$$

In the following, we consider environments characterized by Ohmic-like spectral densities of the form

$$J_s(\omega, \omega_c) = \omega_c \left(\frac{\omega}{\omega_c}\right)^s \exp\left(-\frac{\omega}{\omega_c}\right), \quad (26)$$

where  $\omega_c$  is the cutoff frequency and  $s$  is the Ohmicity parameter. The cutoff frequency is related to the environmental correlation time, and in turn to the decoherence time, whereas  $s$  sets out the behavior of the spectral density in the low-frequency range. Three main classes may be identified: the sub-Ohmic ( $0 < s < 1$ ), the Ohmic ( $s = 1$ ), and the super-Ohmic ( $s > 1$ ) [34,35].

Notice that for a dephasing quantum probe the populations of the energy levels are not changed by the evolution, which affects only the off-diagonal terms of the density matrix of the system. In other words, there is no exchange of energy between the probe and the system under investigation, and the state of the probe is always out of equilibrium.

### B. Out-of-equilibrium qubit probe

Let us first consider a qubit probe. In this case,  $\delta_0 = -1$  and  $\delta_1 = +1$  and we make the identification  $|e_0\rangle \rightarrow |0\rangle$  and  $|e_1\rangle \rightarrow |1\rangle$ . Thus  $\mathcal{R}(t) = \mathbb{I}_2$  and we can write the density matrix (21) directly in the basis  $|i\rangle$  at time  $t$ , obtaining

$$\rho_S^\beta(t) = \begin{bmatrix} 1 & e^{\Gamma(t|\beta)} \\ e^{\Gamma(t|\beta)} & 1 \end{bmatrix} \circ \rho_S. \quad (27)$$

We assume no *a priori* information about the two temperatures to be discriminated, i.e.,  $z_1 = z_2 = 1/2$ . The operator  $\Lambda$



in Eq. (2) may be written as

$$\Lambda = \begin{pmatrix} 0 & \rho_{10} \\ \rho_{01} & 0 \end{pmatrix} \frac{e^{\Gamma(t|\beta_2)} - e^{\Gamma(t|\beta_1)}}{2} \quad (28)$$

where  $\rho_{10}$  and  $\rho_{01}$  are the off-diagonal elements of the initial state of the probe. The probability of error is thus given by

$$p_e^{\text{neq}}(\beta_1, \beta_2) = \frac{1}{2} \left[ 1 - \left| \rho_{10} (e^{\Gamma(t|\beta_2)} - e^{\Gamma(t|\beta_1)}) \right| \right]. \quad (29)$$

We notice that the probability of error depends only on the off-diagonal values of the density matrix at time  $t = 0$  and it does not depend on the value of  $\omega_0$ . Using the Bloch vector formalism, it can be seen that the best preparation is given for  $|\rho_{10}| = 1/2$  and  $\rho_{00} = \rho_{11} = 1/2$ . If  $\rho_{01}$  is real, the optimal probe state is the maximally coherent state  $|\psi_S(0)\rangle = 1/\sqrt{2}(|0\rangle + |1\rangle)$ .

Generally speaking, we can exactly find the optimal POVM to be implemented on the probe, which is identified by the projectors of the  $\Lambda$  operator (28). Indeed, if we write  $\rho_{01} = r e^{-i\alpha}$ , then we can write the projective measurement in terms of Pauli matrices as

$$\Pi_1 = \frac{1}{2} [\mathbb{I} + \cos(\alpha)\sigma_x + \sin(\alpha)\sigma_y], \quad (30)$$

$$\Pi_2 = \frac{1}{2} [\mathbb{I} - \cos(\alpha)\sigma_x - \sin(\alpha)\sigma_y]. \quad (31)$$

This is a feasible POVM which depends on the initial preparation but not on the two temperatures (it does, however, depend on time since the above expression is in the interaction picture).

The above results may be interpreted in terms of coherence of the probe, i.e., the quantity  $\mathcal{C}(\rho) = \sum_{i \neq j} |\rho_{ij}|$ . For the state in Eq. (27), the coherence is

$$\mathcal{C}(\beta, t) = 2|\rho_{01}^0| e^{\Gamma(t|\beta)}, \quad (32)$$

and the probability of error may be written as a function of the coherence only:

$$p_e^{\text{neq}}(\beta_1, \beta_2) = \frac{1}{2} \left[ 1 - \left| \mathcal{C}(\beta_2, t) - \mathcal{C}(\beta_1, t) \right| \right]. \quad (33)$$

Better discrimination is thus obtained for states with larger differences of their coherence. In turn, maximally coherent states are optimal states, since they are more sensible to decoherence, which is the sole effect of the pure dephasing model.

In Fig. 2 we show the probability of error (29) for an Ohmic environment with  $s = 1$  and  $\omega_c = 7$  kHz. We see that for  $T_1 = 1$  mK (upper panel) there is an optimal time at which to perform the measurement. Moreover, the minimum  $p_e^{\text{neq}}$  is minimum when the second temperature  $T_2$  is smaller, as one would expect. Instead, when  $T_1 = 0$  mK (lower panel), there is a large optimal time interval, at least when times are at the order of  $10^{-5}$ . If we were to consider different values of  $s$  and  $\omega_c$ , we would obtain similar shapes of  $p_e^{\text{neq}}$  but different optimal times. Indeed, the optimal time decreases for non-Ohmic environments ( $s \neq 1$ ) or for smaller cutoff frequency  $\omega_c$ . Notice that the value of  $p_e^{\text{neq}}$  does not depend on  $\omega_0$ . This is expected since the model we are considering is a pure dephasing model without energy exchanges.

Finally, in Fig. 3, we compare the performance of the equilibrium probe studied in Sec. III to that of a dephasing

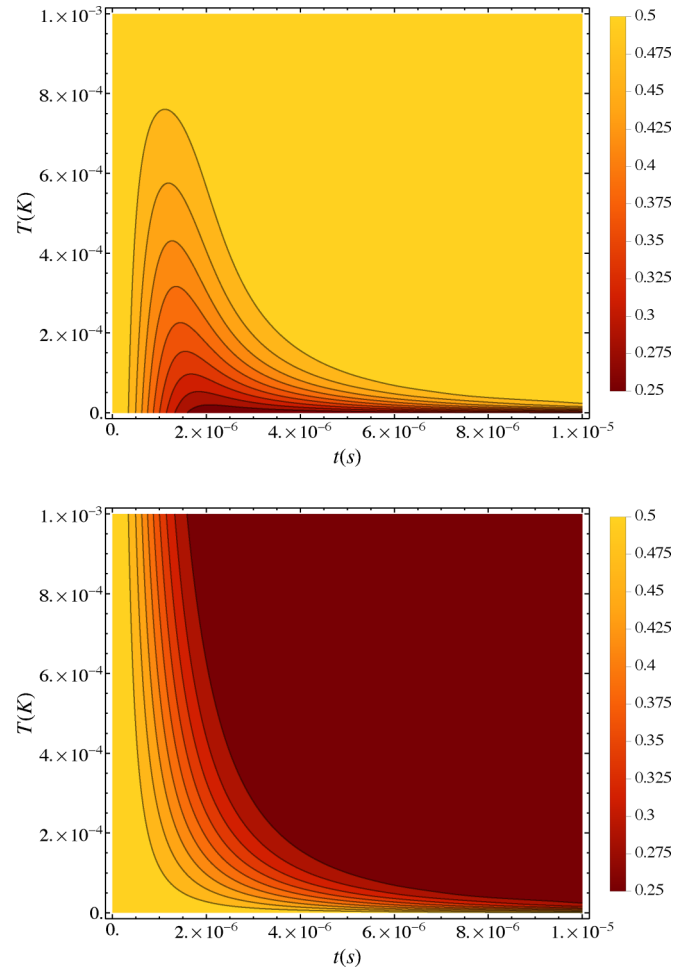


FIG. 2. Probability of error  $p_e^{\text{neq}}(T_1, T_2)$  for a qubit (29) as a function of time  $t$  and  $T_2$  for maximally coherent state  $\rho_{10} = 1/2$ . We fixed  $\omega_c = 7$  kHz and  $s = 1$ . Upper panel:  $T_1 = 1$  mK. Lower panel:  $T_1 = 0$  K.

one. In order to have a faithful comparison, we introduce a gain factor defined as

$$\eta(T_1, T_2) = 1 - \frac{p_e^{\text{neq}}(T_1, T_2)}{p_e^{\text{eq}}(T_1, T_2)}. \quad (34)$$

A positive value of  $\eta(T_1, T_2)$  means that the probability of error in the nonequilibrium regime is lower than the probability of error in the equilibrium regime. Thus  $\eta$  quantifies the gain we obtain with a nonequilibrium probe. In contrast, negative  $\eta$  means that an equilibrium probe provides a lower probability of error, and thus the latter is preferable. We show the gain factor in the upper panel of Fig. 3 for  $T_1 = 1$  mK. We see that there is a threshold time, below which out-of-equilibrium probes outperform equilibrium ones. After that time, out-of-equilibrium and equilibrium probes provide nearly the same performance. The gain factor for  $T_1 = 0$  K is shown in the lower panel of Fig. 3. Here, we see a completely different behavior. The reason lies in the fact that in the limit of  $T_1 \rightarrow 0$  and for  $T_2 \sim 10^{-3}$  we have  $p_e^{\text{eq}} \simeq 1/4$ , i.e., we are in the region where equilibrium probes are optimal.

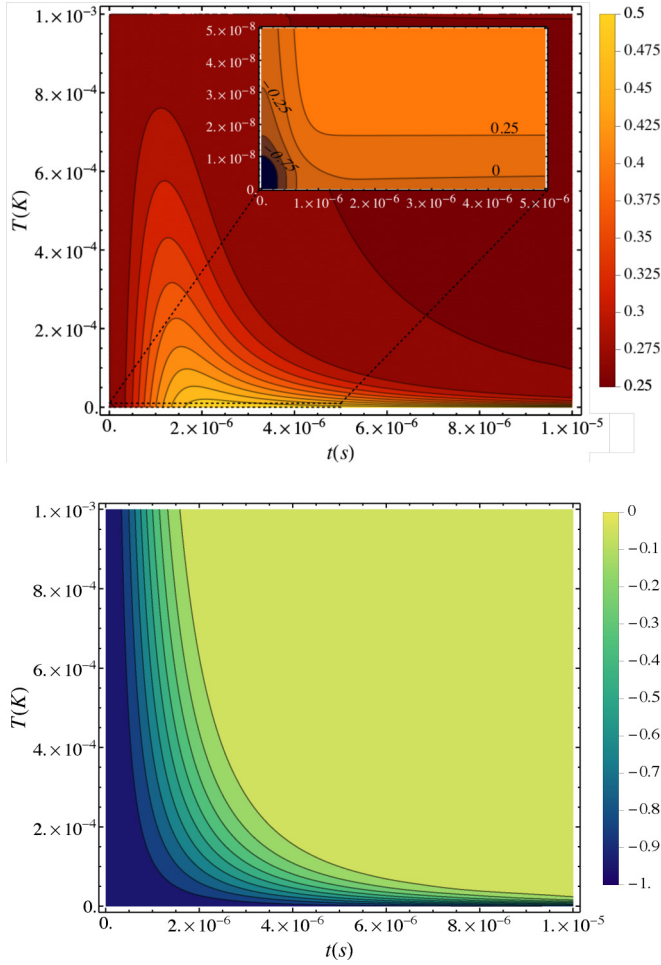


FIG. 3. Gain factor  $\eta$  (equilibrium vs out of equilibrium) given in (34) as a function of time  $t$  and  $T_2$  for the maximally coherent state. We fixed  $\omega_c = 7$  kHz and  $s = 1$ . Further, we plot  $\eta$  for  $T_2 \sim 10^{-8}$  to show that it becomes negative when  $T_2$  approaches zero, according to the lower panel. Upper panel:  $T_1 = 1$  mK. Lower panel:  $T_1 = 0$  K. Notice the different contour scales in the two plots.

### C. Out-of-equilibrium qutrit probe

In this section we devote our attention to a three-level system with equispaced energy levels. In this system,  $\delta_0 = -2$ ,  $\delta_1 = 0$ , and  $\delta_2 = +2$ , and we make the identification  $|e_0\rangle \rightarrow |0\rangle$ ,  $|e_1\rangle \rightarrow |1\rangle$ , and  $|e_2\rangle \rightarrow |2\rangle$ . The reduced dynamics is given by Eq. (18), with the matrix  $\mathcal{V}^\beta(t)$  now given by

$$\mathcal{V}^\beta(t) = \begin{pmatrix} 1 & e^{\Gamma(t|\beta)} & e^{4\Gamma(t|\beta)} \\ e^{\Gamma(t|\beta)} & 1 & e^{\Gamma(t|\beta)} \\ e^{4\Gamma(t|\beta)} & e^{\Gamma(t|\beta)} & 1 \end{pmatrix}. \quad (35)$$

In order to compare results with those obtained with a qubit probe, we consider a qutrit initially prepared in a maximally coherent state  $|\varphi_3\rangle = (|0\rangle + |1\rangle + |2\rangle)/\sqrt{3}$  and in a qubitlike state  $|\varphi_q\rangle = (|0\rangle + |2\rangle)/\sqrt{2}$ .

In the first case, the trace of the operator  $|\Lambda|$  defined in (2) is given by

$$\text{Tr}[|\Lambda|] = \frac{1}{6} |\mathcal{D}_3(t; \beta_1, \beta_2)| \left[ 1 + \sqrt{1 + 8 \left( \frac{\mathcal{D}_2(t; \beta_1, \beta_2)}{\mathcal{D}_3(t; \beta_1, \beta_2)} \right)^2} \right]$$

where we have defined

$$\mathcal{D}_N(t; \beta_1, \beta_2) = e^{(N-1)^2 \Gamma(t|\beta_2)} - e^{(N-1)^2 \Gamma(t|\beta_1)} \quad (36)$$

(sometimes shortened to  $\mathcal{D}_N$ ). The corresponding probability of error  $p_{e3}^{\text{neq}}(T_1, T_2)$  may be then obtained from Eq. (3). The optimal POVM is given by  $\{\Pi_1 = \mathbb{I}_3 - \Pi_2, \Pi_2 = |\lambda_0\rangle\langle\lambda_0|\}$  where

$$|\lambda_0\rangle = \frac{1}{\sqrt{2 + |\alpha|^2}} (|\tilde{e}_0\rangle + \alpha|\tilde{e}_1\rangle + |\tilde{e}_2\rangle) \quad (37)$$

with

$$\alpha = \frac{-4\mathcal{D}_2^2 + \mathcal{D}_3^2 - \mathcal{D}_3 \sqrt{8\mathcal{D}_2^2 + \mathcal{D}_3^2}}{\mathcal{D}_2(3\mathcal{D}_3 + \sqrt{8\mathcal{D}_2^2 + \mathcal{D}_3^2})} \quad (38)$$

and with the modified energy eigenbasis  $|\tilde{e}_j\rangle = e^{\frac{i\epsilon(t)\delta_j^2}{4}} |e_j\rangle$ . Differently from the qubit case, here the optimal POVM is both time and temperature dependent. For the state  $|\varphi_q\rangle$ ,  $p_{e2}^{\text{neq}}$  is instead similar to that of the qubit, i.e.,

$$p_{e2}^{\text{neq}}(\beta_1, \beta_2) = \frac{1}{2} - \frac{|\rho_{10}|}{2} \left| e^{4\Gamma(t|\beta_1)} - e^{4\Gamma(t|\beta_2)} \right|, \quad (39)$$

with the difference that the exponentials have a more rapid decrease. The behavior is thus similar to that of the qubit, but the minimum is achieved at smaller times.

We now compare the probability of error obtained with an equilibrium probe to that obtained for a qutrit initially prepared in a maximally coherent state. The gain factor is defined as

$$\eta_3(T_1, T_2) = 1 - \frac{p_{e3}^{\text{neq}}(T_1, T_2)}{p_{e3}^{\text{eq}}(T_1, T_2)}, \quad (40)$$

and the value for  $T_1 = 1$  mK is shown in the upper panel of Fig. 4. We see a positive gain factor for times smaller than a certain threshold time (which depends on the second temperature  $T_2$ ). The shape of the  $\eta_3$  is similar to that of the qubit  $\eta$ , but the values are larger (see Fig. 3), in particular the contour scale.

In order to highlight this possible enhancement, we compare the probabilities of error obtained with a maximally coherent qubit and a maximally coherent qutrit. The corresponding gain factor is defined as

$$\eta_c(T_1, T_2) = 1 - \frac{p_{e3}^{\text{neq}}(T_1, T_2)}{p_e^{\text{neq}}(T_1, T_2)} \quad (41)$$

and it is shown in the lower panel of Fig. 4. As we expect, there is an improvement in the discrimination task, especially when  $T_2$  is very small. The physical intuition behind this result is that quantum coherence becomes more fragile for increasing dimension, and thus a qutrit probe is more sensitive than a qubit one.

### D. Out-of-equilibrium equispaced qudit with dimension $N$

We consider now a qudit with generic dimension  $N$  prepared in a maximally coherent state  $\rho_S = 1/N \mathbb{J}_N$ , where  $\mathbb{J}_N$  is

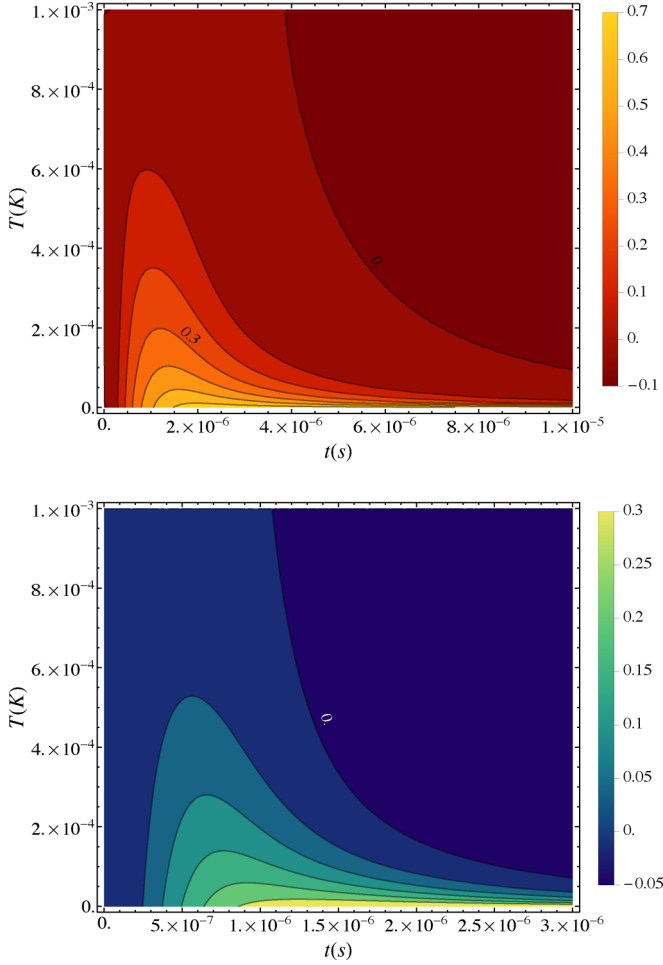


FIG. 4. Upper panel: Gain factor  $\eta_3$  (equilibrium vs out of equilibrium) given in (40). Lower panel: Gain factor  $\eta_c$  (qubit vs qutrit) given in (41). Both are a function of time  $t$  and  $T_2$ . We fixed  $\omega_c = 7$  kHz,  $s = 1$ , and  $T_1 = 1$  mK. Notice the different time scales and the different contour scales in the two panels.

the  $N$ -dimensional matrix of ones. In this case the  $\Lambda$  is

$$\begin{aligned} \Lambda &= \frac{1}{2N} (\mathcal{V}^{\beta_2}(t) - \mathcal{V}^{\beta_1}(t)) \circ \mathcal{R}(t) \\ &= \frac{1}{2N} \sum_{jk} \left( e^{\frac{(\delta_j - \delta_k)^2}{4} \Gamma(t|\beta_2)} - e^{\frac{(\delta_j - \delta_k)^2}{4} \Gamma(t|\beta_1)} \right) |\tilde{e}_j\rangle \langle \tilde{e}_k| \end{aligned} \quad (42)$$

where we have defined the modified energy eigenbasis  $|\tilde{e}_j\rangle = e^{\frac{i\xi(t)\delta_j^2}{4}} |e_j\rangle$ . Assuming that the optimal regime is when  $\Gamma(t|\beta_1) \ll 0$  and  $\Gamma(t|\beta_2) \simeq 0$ , we have that the operator  $\Lambda$  in the modified basis is

$$\Lambda \simeq \frac{1}{2N} \begin{pmatrix} 0 & 1 & \cdots & 1 \\ 1 & 0 & \cdots & 1 \\ \vdots & \vdots & \ddots & \vdots \\ 1 & 1 & \cdots & 0 \end{pmatrix}. \quad (43)$$

Under these conditions, the trace of  $|\Lambda|$  is equal to  $1 - 1/N$  and as a result

$$p_{e,N}^{\text{neq}} \geq \frac{1}{2N}, \quad (44)$$

which is the same scaling as that of the equilibrium probe [see (9)]. Nevertheless, from the comparison between equilibrium and out-of-equilibrium probes (see Fig. 3 and upper panel in Fig. 4), a slight enhancement is still possible, due to the different value of the parameter in which the lower bounds (9) and (44) are achieved. Furthermore, in the region where the lower bound is attained, if the dimensions are  $N_1$  and  $N_2$ , we obtain

$$\eta_c^{N_1, N_2}(T_1, T_2) = 1 - \frac{p_{eN_1}^{\text{neq}}(T_1, T_2)}{p_{eN_2}^{\text{neq}}(T_1, T_2)} \simeq 1 - \frac{N_2}{N_1}. \quad (45)$$

In the case of qubit vs qutrit  $\eta_c^{3,2}(T_1, T_2) \simeq 1/3$ , matching the maximum  $\eta_c$  we see in the lower panel of Fig. 4.

Concerning the optimal POVM, we can see that the latter can be approximated by the projectors  $\{\Pi_1 = \mathbb{I}_N - \Pi_2, \Pi_2 = |\lambda_0\rangle \langle \lambda_0|\}$  where

$$|\lambda_0\rangle = \frac{1}{\sqrt{N}} \sum_{i=0}^N |\tilde{e}_i\rangle. \quad (46)$$

Notice that the POVM depends on time  $t$ , which is encoded in phase factor  $\xi(t)$ , but not on temperatures  $\beta_1$  and  $\beta_2$ .

#### E. Out-of-equilibrium quantum register made of two qubits

Now, we investigate the performance of a quantum register of two qubits interacting locally with the thermal bath [19,33]. In this case the matrix of the levels spacing is given by

$$\mathcal{H}^{(2,2)} = (\sigma_3 \otimes \mathbb{I}_2 + \mathbb{I}_2 \otimes \sigma_3). \quad (47)$$

We thus obtain that  $\delta_{00} = -2$ ,  $\delta_{01} = 0 = \delta_{10}$ , and  $\delta_{11} = +2$  and make the identifications  $|e_0\rangle \rightarrow |00\rangle$ ,  $|e_1\rangle \rightarrow |01\rangle$ ,  $|e_2\rangle \rightarrow |10\rangle$ , and  $|e_3\rangle \rightarrow |11\rangle$ . The reduced dynamics is given by Eq. (18), with the matrix  $\mathcal{V}^\beta(t)$  now given by

$$\mathcal{V}^\beta(t) = \begin{pmatrix} 1 & e^{\Gamma(t|\beta)} & e^{\Gamma(t|\beta)} & e^{4\Gamma(t|\beta)} \\ e^{\Gamma(t|\beta)} & 1 & 1 & e^{\Gamma(t|\beta)} \\ e^{\Gamma(t|\beta)} & 1 & 1 & e^{\Gamma(t|\beta)} \\ e^{4\Gamma(t|\beta)} & e^{\Gamma(t|\beta)} & e^{\Gamma(t|\beta)} & 1 \end{pmatrix}. \quad (48)$$

For the register initially prepared in a maximally coherent state  $|\varphi_4\rangle = \frac{1}{4} \sum_k |e_k\rangle$  we have

$$\begin{aligned} \text{Tr}[|\Lambda|] &= \frac{1}{8} |\mathcal{D}_3(t; \beta_1, \beta_2)| \\ &\times \left[ 1 + \sqrt{1 + 16 \left( \frac{\mathcal{D}_2(t; \beta_1, \beta_2)}{\mathcal{D}_3(t; \beta_1, \beta_2)} \right)^2} \right]. \end{aligned} \quad (49)$$

The corresponding probability of error  $p_{e4}^{\text{neq}}(T_1, T_2)$  may be then obtained from Eq. (3). Consequently the POVM is given by  $\{\Pi_1 = \mathbb{I}_4 - \Pi_2, \Pi_2 = |\lambda_0\rangle \langle \lambda_0|\}$  where

$$|\lambda_0\rangle = \frac{1}{\sqrt{2 + 2|\gamma|^2}} (|\tilde{e}_0\rangle + \gamma |\tilde{e}_1\rangle + \gamma |\tilde{e}_2\rangle + |\tilde{e}_3\rangle) \quad (50)$$

with

$$\gamma = \frac{\mathcal{D}_2(3\mathcal{D}_3 + \sqrt{16\mathcal{D}_2^2 + \mathcal{D}_3^2})}{4\mathcal{D}_2^2 + \mathcal{D}_3^2 + B\sqrt{16\mathcal{D}_2^2 + \mathcal{D}_3^2}}. \quad (51)$$

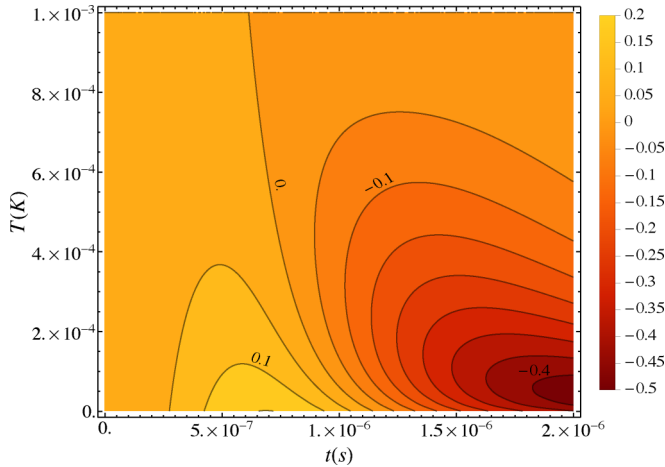


FIG. 5. Gain factor  $\eta_e$  (maximally coherent vs entangled probes) given in (52) as a function of time  $t$  and  $T_2$ . We fixed  $\omega_c = 7$  kHz and  $s = 1$  and  $T_1 = 1$  mK.

Again, the optimal POVM depends both on time  $t$  and on temperatures  $\beta_1$  and  $\beta_2$ .

Moreover, having at one's disposal two qubits, one may wonder whether entanglement may play a role in the discrimination task. We thus consider the four Bell states as possible initial preparation of the probe register. As it may be easily seen, the states  $|\Psi^\pm\rangle = 1/\sqrt{2}(|01\rangle \pm |10\rangle)$  are useless since they are invariant under dynamics (48). Concerning the states  $|\Phi^\pm\rangle = 1/\sqrt{2}(|00\rangle \pm |11\rangle)$  the probability of error  $p_{\Phi^\pm}^{\text{neq}}$  is equal to that of the qutrit (39) prepared in the state  $|\varphi_q\rangle$ .

In order to evaluate whether entanglement is a resource or not in the discrimination task, we compare the error probability obtained with a maximally coherent probe with that obtained with the Bell state  $|\Phi^+\rangle$  by the factor

$$\eta_e(T_1, T_2) = 1 - \frac{p_{\Phi^+}^{\text{neq}}(T_1, T_2)}{p_{e4}^{\text{neq}}(T_1, T_2)}. \quad (52)$$

In Fig. 5, we clearly see a threshold time that splits the plot into two parts: in the first, at smaller times, entangled probes lead to a lower probability of error. In the second region, i.e., for larger times, maximally coherent probes outperform entangled ones. In the next section, we will explore in detail the performance of entangled probes, thus providing an explanation of why entangled states are better probes at smaller times. The implementation of the optimal POVM will be also discussed.

### F. Out-of-equilibrium entangled states in a quantum register of $N$ qubits

Finally, we explore the performance of entangled states in a  $N$ -dimensional quantum register.

First, let us consider  $N$ -dimensional Greenberger-Horne-Zeilinger (GHZ) states  $|\text{GHZ}_N\rangle = \frac{1}{\sqrt{2}}(|0 \cdots 0\rangle + |1 \cdots 1\rangle)$ . In the basis  $|\tilde{e}_j\rangle$  we have that

$$\Lambda = \frac{1}{4} \begin{pmatrix} 0 & \cdots & \mathcal{D}_N(t; \beta_1, \beta_2) \\ \vdots & \ddots & \vdots \\ \mathcal{D}_N(t; \beta_1, \beta_2) & \cdots & 0 \end{pmatrix}. \quad (53)$$

It is straightforward to see that

$$p_e^{\text{neq}}(\beta_1, \beta_2; N) = \frac{1}{2} \left( 1 - \frac{|\mathcal{D}_N(t; \beta_1, \beta_2)|}{2} \right). \quad (54)$$

The probability of error has the same form as that of the qubit, with the only difference in the prefactor of  $\Gamma(t|\beta)$ , which results only in a rescaling of the optimal time, as it has been discussed for the quantum register of two qubits. The optimal POVM is given by  $\{\Pi_1 = |\text{GHZ}_N\rangle\langle\text{GHZ}_N|, \Pi_2 = \mathbb{I}_{2N} - \Pi_1\}$  and it is time and temperature independent. In addition, we notice that in the optimal region  $\Gamma(t|\beta_1) \ll 0$  and  $\Gamma(t|\beta_2) \simeq 0$  we have that  $p_e^{\text{neq}} \geq 1/4$ , so there is no scaling advantage in term of dimension  $N$ .

Secondly, we consider  $W$  states, i.e.,  $|W_N\rangle = 1/\sqrt{N}(|10 \cdots 0\rangle + |01 \cdots 0\rangle + \dots + |0 \cdots 01\rangle)$ . All the elements in the superposition have the same energy, so the state is stationary [see (21)]. Thus, there is no dephasing in the state and consequently the probability of error is maximum  $p_e^{\text{neq}} = 1/2$ .

## V. CONCLUSION

In this paper, we have analyzed in detail the use of quantum probes to discriminate two structured baths at different temperatures. In particular, we have addressed quantum probes interacting with their environment by a dephasing Hamiltonian and compared the discrimination performance with those of equilibrium probes.

At first, we have addressed the discrimination problem for an equilibrium probe and evaluated the probability of error, showing that energy measurement is optimal in this regime. We have then moved to out-of-equilibrium dephasing probes, and derived the exact reduced dynamics for a finite quantum system locally interacting with an Ohmic-like thermal bath. Upon exploiting this result, we have studied the behavior of the probability of error as a function of the interaction time and found that in the low-temperature regime out-of-equilibrium probes outperform equilibrium ones at finite times. We also found that there is a finite value of the interaction time minimizing the probability of error. In turn, it results that for qubit systems maximally coherent states generally represent the best preparation of the probe for the discrimination task. On the other hand, when one of the two temperatures is zero, equilibrium probes may represent the optimal choice. For maximally coherent qubit probes, we have obtained the optimal POVM, which is a spin measurement along the  $x$  axis. Remarkably, this POVM is independent of time and temperatures (except for the free evolution phase factor). Instead, for maximally coherent qudits of dimension  $N$ , we found that under some conditions there is an optimal region where the minimum probability of error scales as  $1/2N$ . In general, for qudits, the optimal POVM is time and temperatures dependent, but the temperature dependency disappears in the optimal region.

We have compared qubit probes with qutrit ones, and have shown numerically that qutrits allow one to achieve lower error probability. Finally, we have also investigated the role of entanglement, showing that at variance with maximally coherent probes there is no scaling in the minimum of the probability of error, but only a decrease in the optimal time



scale. Moreover, the optimal POVM for GHZ states does not depend on the temperatures. Overall, we conclude that the optimal POVM may be easily implemented for qubit and GHZ probes, whereas it may be more challenging to realize in practice optimal discrimination with higher dimensional probes.

Our results indicate that dephasing quantum probes are useful for the task of discriminating temperatures at intermediate interaction times, and that out-of-equilibrium

coherent quantum probes represent a resource not only for quantum estimation but also for quantum discrimination.

#### ACKNOWLEDGMENT

The authors thank C. Benedetti, M. Bina, and S. Razavian for useful discussions. M.G.A.P. is a member of GNFM-INdAM.

- 
- [1] M. Mehboudi, A. Sanpera, and L. A. Correa, *J. Phys. A: Math. Theor.* **52**, 303001 (2019).
  - [2] A. De Pasquale and T. M. Stace, in *Thermodynamics in the Quantum Regime* (Springer, New York, 2018), pp. 503–527.
  - [3] P. P. Potts, J. B. Brask, and N. Brunner, *Quantum* **3**, 161 (2019).
  - [4] M. G. A. Paris, *J. Phys. A: Math. Theor.* **49**, 03LT02 (2015).
  - [5] M. Bruderer and D. Jaksch, *New J. Phys.* **8**, 87 (2006).
  - [6] T. M. Stace, *Phys. Rev. A* **82**, 011611(R) (2010).
  - [7] M. Brunelli, S. Olivares, and M. G. A. Paris, *Phys. Rev. A* **84**, 032105 (2011).
  - [8] M. Brunelli, S. Olivares, M. Paternostro, and M. G. A. Paris, *Phys. Rev. A* **86**, 012125 (2012).
  - [9] U. Marzolino and D. Braun, *Phys. Rev. A* **88**, 063609 (2013).
  - [10] K. D. B. Higgins, B. W. Lovett, and E. M. Gauger, *Phys. Rev. B* **88**, 155409 (2013).
  - [11] M. Mehboudi, M. Moreno-Cardoner, G. D. Chiara, and A. Sanpera, *New J. Phys.* **17**, 55020 (2015).
  - [12] M. Jarzyna and M. Zwierz, *Phys. Rev. A* **92**, 032112 (2015).
  - [13] A. D. Pasquale, D. Rossini, R. Fazio, and V. Giovannetti, *Nat. Commun.* **7**, 12782 (2016).
  - [14] M. R. Jørgensen, P. P. Potts, M. G. A. Paris, and J. B. Brask, *Phys. Rev. Research* **2**, 033394 (2020).
  - [15] L. A. Correa, M. Mehboudi, G. Adesso, and A. Sanpera, *Phys. Rev. Lett.* **114**, 220405 (2015).
  - [16] L. Mancino, M. G. Genoni, M. Barbieri, and M. Paternostro, *Phys. Rev. Research* **2**, 033498 (2020).
  - [17] P. P. Hofer, J. B. Brask, M. Perarnau-Llobet, and N. Brunner, *Phys. Rev. Lett.* **119**, 090603 (2017).
  - [18] S. Razavian, C. Benedetti, M. Bina, Y. Akbari-Kourbolagh, and M. G. Paris, *Eur. Phys. J. Plus* **134**, 284 (2019).
  - [19] F. Gebbia, C. Benedetti, F. Benatti, R. Floreanini, M. Bina, and M. G. A. Paris, *Phys. Rev. A* **101**, 032112 (2020).
  - [20] S. Jevtic, D. Newman, T. Rudolph, and T. M. Stace, *Phys. Rev. A* **91**, 012331 (2015).
  - [21] I. Gianani, D. Farina, M. Barbieri, V. Cimini, V. Cavina, and V. Giovannetti, *Phys. Rev. Research* **2**, 033497 (2020).
  - [22] S. Razavian and M. G. Paris, *Physica A* **525**, 825 (2019).
  - [23] A. Chefles, *Contemp. Phys.* **41**, 401 (2000).
  - [24] J. A. Bergou, U. Herzog, and M. Hillery, in *Quantum State Estimation*, edited by M. Paris and J. Řeháček (Springer-Verlag, Berlin, 2004), pp. 417–465.
  - [25] S. M. Barnett and S. Croke, *Advances in Optics and Photonics* **1**, 238 (2009).
  - [26] J. Bae and L.-C. Kwek, *J. Phys. A: Math. Theor.* **48**, 083001 (2015).
  - [27] C. W. Helstrom, *J. Stat. Phys.* **1**, 231 (1969).
  - [28] J. A. Bergou, *J. Phys.: Conf. Ser.* **84**, 012001 (2007).
  - [29] M. A. Nielsen and I. L. Chuang, *Quantum Computation and Quantum Information*, 10th ed. (Cambridge University Press, 2011).
  - [30] Q. Bouton, J. Nettersheim, D. Adam, F. Schmidt, D. Mayer, T. Lausch, E. Tiemann, and A. Widera, *Phys. Rev. X* **10**, 011018 (2020).
  - [31] H.-P. Breuer, E.-M. Laine, J. Piilo, and B. Vacchini, *Rev. Mod. Phys.* **88**, 021002 (2016).
  - [32] H.-P. Breuer and F. Petruccione, *The Theory of Open Quantum Systems* (Oxford University, New York, 2002).
  - [33] J. H. Reina, L. Quiroga, and N. F. Johnson, *Phys. Rev. A* **65**, 032326 (2002).
  - [34] A. J. Leggett, S. Chakravarty, A. T. Dorsey, M. P. A. Fisher, A. Garg, and W. Zwerger, *Rev. Mod. Phys.* **59**, 1 (1987).
  - [35] A. Shnirman, Y. Makhlin, and G. Schön, *Phys. Scr.* **T102**, 147 (2002).